

Metastable tetragonal states of zirconium: Theory and experiment

X. Z. Ji, F. Jona, and P. M. Marcus

Department of Materials Science and Engineering, State University of New York, Stony Brook, New York 11794-2275, USA

(Received 3 March 2003; published 29 August 2003)

The epitaxial Bain path of tetragonal zirconium has been calculated with the full-potential linearized-augmented-plane-wave method within both the nonrelativistic local-density approximation (LDA) and the relativistic generalized-gradient approximation (GGA). Both procedures yield three energy minima, corresponding to three tetragonal phases with different axial ratios c/a . For the LDA the three phases are face-centered cubic (fcc), body-centered cubic (bcc), and body-centered tetragonal (bct); all three are metastable, as determined by calculations of the corresponding elastic constants. For the GGA the three phases are fcc and two bct (the bcc phase is at a maximum and unstable). Experiments were carried out with the goal of stabilizing the fcc phase by pseudomorphic epitaxy of zirconium films on a {001} surface of tungsten. The structure of the zirconium films was determined by quantitative low-energy electron diffraction and found to be strained fcc, strained by the pseudomorphism. Agreements and disagreements with published results of other workers are discussed.

DOI: 10.1103/PhysRevB.68.075421

PACS number(s): 68.55.Nq, 64.70.Kb, 64.60.My, 61.66.Bi

I. INTRODUCTION

The ground state of Zr at room temperature and atmospheric pressure is hexagonal close packed (hcp), and becomes body-centered cubic (bcc) at temperatures higher than about 1133 K.¹ However, two partially contradictory reports^{2,3} describe the growth of a face-centered-cubic (fcc) phase of Zr in the form of relatively thick films. Chopra, Randlett, and Duff² (CRD) used transmission and reflection electron diffraction, as well as x rays, to study Zr films sputtered or evaporated on different substrates. The experiments were done in a relatively poor (by today's standards) vacuum of 10^{-6} Torr and at rather fast deposition rates (~ 200 Å/min). Deposition on room-temperature substrates reportedly produced amorphous films and deposition at 200 °C–400 °C produced fcc Zr, which was found to be present even in films as thick as 2 μm , although thicker films had mixtures of fcc and hcp Zr. The fcc phase was formed on all three types of substrates used: glass, mica, and rocksalt. The lattice constant of the conventional cell of fcc Zr was determined to be $a_0 = 4.61$ Å, the corresponding body-centered-tetragonal (bct) unit cell would therefore have a primitive square base with sides $a = 4.61/\sqrt{2} = 3.26$ Å.

A later paper by Hill *et al.*³ describes the growth of Zr films evaporated on a W{001} substrate in ultrahigh vacuum and studied by both reflection high-energy electron diffraction and low-energy electron diffraction (LEED), but not by LEED intensity analysis. In contrast to CRD, deposition of Zr on a 300-K substrate produced crystalline films, which were and remained 1×1 with $a = 3.16$ Å up to thicknesses of 50 atomic layers, and even after anneals to 1300 K. The authors added that “deposits between 10 and 50 monolayers annealed to 1300–1800 K” formed islands that grew “smoothly out of the 1×1 layer”³ and were found to be fcc with $a_0 = 4.63$ Å, i.e., $a = 3.27$ Å, in agreement with CRD. The fcc islands were stable up to 1800 K, in contrast to CRD, who found that above 700 K the structure reverted to hcp Zr.

Stabilization of metastable fcc phases of hcp crystals is

not uncommon, e.g., Ti/Al{001} (Ref. 4) and Mg/W{001},⁵ but requires constraining the growing film on a suitable substrate in pseudomorphic growth in which the film unit mesh is strained to the substrate unit mesh. What is surprising about the CRD results mentioned above is that the fcc modification of Zr, which does not appear in the phase diagram at any temperature, can be formed without constraints (i.e., not pseudomorphically) on substrates with different unit meshes and even on amorphous substrates, and persists in rather thick films up to very high temperatures.

To clarify the energetics of all possible tetragonal phases of Zr metal we have calculated the corresponding epitaxial Bain path (EBP), and we report here the results. The EBP, we recall, is a unique path that goes through all epitaxially strained states, which includes all tetragonal energy minima. The energy minima are the states that can be tetragonal metastable phases of any given crystal.⁶ A convenient form of the EBP is a plot of the total energy per atom versus the ratio c/a of the tetragonal lattice parameters (a for the square base and c for the height of the two-atom bct cell). The minima of energy identify equilibrium states, which may be stable, metastable, or unstable, depending on whether the corresponding elastic constants satisfy the stability conditions.⁶ A standard model of the EBP has two minima and a maximum of energy between them; the minima correspond either to dominant binding *between* (001) planes (small c/a) or to dominant binding *within* (001) planes (large c/a). At both small and large c/a the energy increases rapidly, since atoms begin to overlap, hence the energy must have at least one minimum.

We show below that the EBP of tetragonal Zr does not conform to the standard model in that it has *three* energy minima, separated by energy maxima. We find that the bcc phase of Zr is stable in one mode of calculation [local-density approximation (LDA)] and unstable in another [generalized-gradient approximation (GGA)] (see below), while the fcc phase is metastable in both modes. We also have done, and describe below, experiments aimed at stabi-

lizing fcc Zr by pseudomorphic epitaxy on a $W\{001\}$ substrate.

The organization of this report is as follows. Section II presents details of the calculations of the EBP and of elastic constants of three phases, and Sec. III summarizes the results. Section IV describes the experiments and the intensity analysis. Section V presents a discussion of the results.

II. CALCULATIONS

The procedures for the calculation of EBP's have been described elsewhere;⁷ they require a total-energy electronic-structure computer program. We used the WIEN97 program, which applies the full-potential linearized-augmented-plane wave to calculations of total energies for a variety of crystal structures and space groups.⁸ The program allows a choice of nonrelativistic (NREL) or relativistic (RELA) calculations in either the LDA or the GGA. The program was implemented and executed on a LINUX-based desktop personal computer. The calculations for the EBP were done with both the NREL-LDA and the RELA-GGA formulations. In both cases a large plane-wave cutoff of $RK_{\max}=9$ was used (resulting in 500 to 550 plane waves), as well as a k -point sampling of 12 000 points in the full Brillouin zone, corresponding to 800 to 1500 k points in the irreducible wedge of the Brillouin zone; a criterion of 1×10^{-6} Ry was used for energy convergence.

The determination of the elastic constants of tetragonal states, which requires calculations of the total energy of appropriately strained modifications of those states, was done only with the NREL-LDA. The procedures followed for the calculation of elastic constants are described in detail elsewhere.⁶

III. RESULTS

Figure 1 depicts three forms of the EBP of bct Zr as calculated with both NREL-LDA (solid lines) and RELA-GGA (dashed lines). The upper panel is a plot of the lattice constant c versus the axial ratio c/a ; this plot is useful for finding the lattice parameters of any bct phase at given c/a .

The middle panel shows the normalized energy per atom $E-E_0$ (E_0 is the smallest energy found on the tetragonal EBP) as a function of c/a . We note (i) there are three energy minima for both NREL-LDA and RELA-GGA, which, as mentioned above, is a deviation from the standard EBP model. (ii) Both the LDA and the GGA agree on producing a local energy minimum at $c/a \sim \sqrt{2}$, which corresponds to an fcc phase, but do not agree on the other two minima. At $c/a=1$, which denotes a bcc phase, the LDA has a local minimum, but the GGA has a local *maximum*: hence, for the GGA, bcc Zr is unstable. (iii) The LDA calculation finds another energy minimum at $c/a=0.795$, while the GGA finds two additional energy minima, one at $c/a=0.807$ and another at $c/a=0.854$. (iv) For the GGA the fcc phase has the lowest-energy minimum, while for the LDA it has the highest. For each phase, the lattice parameters, the axial ratio, the volume per atom, and the corresponding total energy per atom are given in Table I.

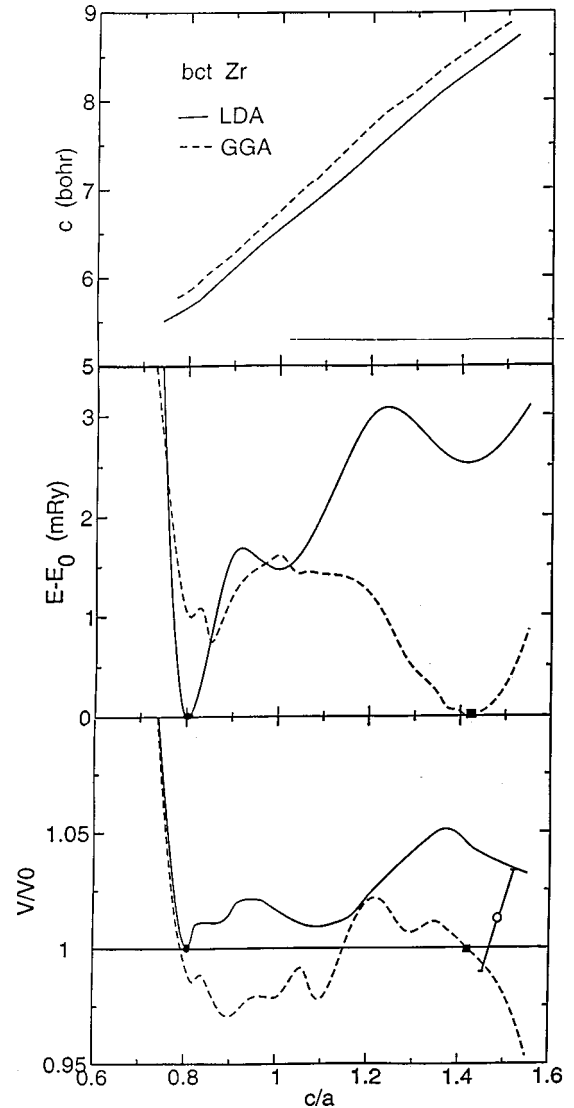


FIG. 1. Epitaxial Bain path of tetragonal zirconium. Top: tetragonal c parameter versus axial ratio c/a . Middle: Total energy per atom E referred to the energy E_0 of the lowest-energy state versus c/a . Bottom: Relative volume V/V_0 (V_0 =volume per atom of the calculated fcc unit cell). The filled circle and square mark the positions of the lowest-energy states for the LDA and GGA, respectively. The open circle marks the experimental result discussed in Secs. IV and V.

The bottom panel of Fig. 1 depicts the normalized volume V/V_0 along the EBP (V_0 is the volume per atom of the lowest-energy tetragonal phase). This plot is useful for the assignment of experimentally determined phases, as is discussed below.

The elastic constants have been calculated for the three phases corresponding to energy minima in the NREL-LDA calculation: fcc, bcc, and bct. The results are listed in Table I. For all three phases the shear modulus $C' \equiv (c_{11} - c_{12})/2$ and the shear constant c_{44} are found to be positive. In addition the shear constant c_{66} of the bct phase is also found to be positive. These results indicate that all three phases are metastable in the LDA. We have not calculated the elastic constants, and hence have not tested the stability of the three

TABLE I. Lattice parameters and elastic constants of fcc and bcc Zr. a and c are the parameters of the bcc unit cell, in Å units; V is the volume per atom, in Å³; E is the total energy per atom and E^+ is the reduced energy per atom, in Ry ($E^+ = E + 7074$ for the LDA and $E^+ = E + 7198$ for the GGA); c_{ij} are elastic constants, in Mb; $C' \equiv (c_{11} - c_{12})/2$ is the shear modulus, in Mb.

	fcc Zr		bcc Zr		bct Zr		bct Zr	
	LDA	GGA	LDA	GGA	LDA	GGA	LDA	GGA
a	3.121	3.216	3.469	3.580	3.730	3.856	3.774	
c	4.405	4.529	3.470	3.568	2.967	3.111	3.224	
c/a	1.411	1.408	1.000	0.997	0.795	0.807	0.854	
V	21.45	23.42	20.87	22.86	20.64	23.13	22.96	
E^+	-0.044 405	-0.432 660	-0.045 457	-0.429 445	-0.047 066	-0.430 658	-0.431 165	
c_{11}	1.109		1.087		1.303			
c_{12}	0.612		0.854		0.868			
C'	0.247		0.233		0.434			
c_{44}	0.461 ^a		0.106		0.393			
c_{66}	0.461		0.106		0.203			

^aThe c_{44} constant of fcc crystals can be calculated in two ways (which do not give quite the same results, probably due to limited calculation accuracy): $c_{44}^{dir} = c'_{44}$ and $c_{44}^{ind} = c'_{11} - c'_{33} + c'_{66}$, where c'_{ij} are the elastic constants of the bct cell of the fcc lattice, i.e., the elastic constants in tetragonal axes (Ref. 7). Here $c_{44}^{dir} = 0.461$ and $c_{44}^{ind} = 0.514$.

phases found on the GGA EBP.

IV. LEED EXPERIMENTS AND INTENSITY ANALYSIS

A. Experiments

The calculated lattice constants of the bct cell of fcc Zr, averaged between LDA and GGA results (see Table I), are $a = 3.17$ and $c = 4.47$ Å, in reasonable agreement with the experimental data reported by CRD (Ref. 2) and Hill *et al.*³ Our calculations indicate that this phase is metastable, hence it is a good candidate for stabilization by pseudomorphic epitaxy on a suitable substrate. We have done experiments to achieve such a stabilization.

A suitable substrate for these experiments is a W{001} surface, which has a square net (W is bcc) with $a = 3.1652$ Å (hence with a misfit of only 0.15%). We obtained a platelet of pure tungsten ($8 \times 9 \times 0.5$ mm³) with one major surface oriented parallel to {001} within about 0.5°. We mounted the platelet in an experimental chamber pumped by a 500-l/sec sputter-ion pump and provided with LEED optics and an additional electron gun for Auger-electron spectroscopy (AES). The W{001} surface was cleaned with sequences of argon-ion bombardments (in 5×10^{-5} Torr of Ar gas, with 200-eV ions and current densities of about 2 $\mu\text{A}/\text{cm}^2$) followed by annealing treatments (typically 30 min at about 1200 °C). These treatments produced a W surface on which AES revealed no impurities above the noise, and LEED showed a sharp-spot 1×1 low-background pattern.

The source for Zr deposition was a 99.8%-pure Zr wire which was heated by electric current, usually to temperatures around 1500 °C. Deposition rates were kept slow, the deposition times varying between 10 and 30 min, corresponding to rates between 0.05 and 0.2 Å/min. Film thickness was estimated from the ratio of AES lines: Zr at 147 eV to W at 169 eV, but for thicker films (about 40 Å) the W AES lines were too small to be measured reliably. In any case, the accuracy of film-thickness determination was poor, probably

around $\pm 50\%$. In the initial stages the W substrate was not heated during deposition of Zr; in later stages the substrate was heated to about 200 °C.

The experiments involved repetitions of the following sequence: (i) small deposition of Zr; (ii) AES scan to estimate the surface coverage; (iii) LEED observation of the geometry and quality of the pattern; (iv) collection of intensity-versus-voltage [$I(V)$] curves. This sequence was repeated as long as the LEED pattern from the Zr film was visible and the $I(V)$ curves were measurable over the background, then the film was sputtered away, the W substrate recleaned, and the sequence started again.

After all depositions the LEED pattern remained 1×1 and geometrically identical to the pattern of clean W{001}, showing that the growing Zr film was pseudomorphic. But the background increased with increasing film thickness, and the $I(V)$ spectra changed until the Zr film reached about 15-to 20-Å thickness, after which the spectra became stable (indicating that the incident electrons did not reach the film-substrate interface). One series of $I(V)$ curves were collected from a Zr film grown on the unheated substrate, a second series from a Zr film grown on the unheated substrate and then annealed at 200 °C for 30 min, and a third series from a Zr film grown on the substrate heated to about 200 °C. The $I(V)$ curves in the second and third series were practically identical to one another, and both were different from those in the first series. The curves used in the analyses described below stemmed from Zr films with thickness estimated to be about 40 Å (the W signal was no longer visible in AES scans).

B. Intensity analysis

Films thick enough to produce stable $I(V)$ curves were considered semi-infinite for the purpose of LEED intensity analysis. The calculations of diffracted intensities were done with the CHANGE computer program written by Jepsen,⁹ including 69 beams and 5 phase shifts up to 360 eV. The Zr

potential was obtained from the collection of Moruzzi, Janak, and Williams.¹⁰ The real part of the inner potential was initially set at 10 eV and was adjustable during the analysis; the imaginary part was 4 eV and the root-mean-square amplitude of thermal vibrations was $(\langle u^2 \rangle)^{1/2} = 0.1328 \text{ \AA}$.

The in-plane lattice constant of the Zr film was set equal to that of W{001}, $a = 3.1652 \text{ \AA}$, as required by the pseudomorphism. The calculations were done for many values of the bulk interlayer spacing d_{bulk} : from 1.20 to 2.70 \AA , initially in steps of 0.1 \AA , and later in steps of 0.05 and even 0.01 \AA , in each case varying the *change* in the first interlayer spacing Δd_{12} from -0.5 to $+0.5 \text{ \AA}$ in steps of 0.05 \AA . The $I(V)$ curves calculated for each d_{bulk} value were compared with the experimental curves both visually and by calculation of the Zanazzi-Jona (ZJ) R factor r_{ZJ} .¹¹ For the best parameters thus found we then tested possible changes Δd_{23} in the second interlayer spacing.

We first considered the $I(V)$ curves of the Zr films grown on the unheated substrate. We were unable to find a suitable theoretical match within the range of d_{bulk} values listed above. Several attempts at testing the possibility of Zr-W or Zr-C mixtures (in some cases, especially after long exposure times, a C signal was detectable in AES scans) also failed. We have no explanation for these failures: the growth was certainly pseudomorphic, hence the a parameter was known, but no interlayer spacings were found that would fit the experimental data.

However, the $I(V)$ curves of Zr films grown on the heated substrate, or deposited on the unheated substrate and then annealed to about 200 $^{\circ}\text{C}$, could be fitted by calculations, but the high background in the LEED pattern complicated the R -factor analysis considerably, thus producing rather large error bars. The best agreement between calculated and observed $I(V)$ curves was found for the following parameters (lengths in \AA):

$$d_{\text{bulk}} = 2.35 \pm 0.05, \quad \Delta d_{12} = -0.17 \pm 0.05,$$

$$\Delta d_{23} = -0.05 \pm 0.06, \quad r_{\text{ZJ}} = 0.19.$$

Both calculated and observed $I(V)$ curves are depicted in Fig. 2.

V. DISCUSSION

Although the fit to experiment of the calculated $I(V)$ curves is only mediocre (subtraction of the high background is a difficult task to carry out accurately), the R factor was clearly a minimum for the curves depicted in Fig. 2. It is therefore appropriate to conclude that the parameters listed above describe well, within the error bars, the Zr film under scrutiny. It is clear that the film is strained from some phase that is forced to assume the in-plane lattice constant of the substrate surface. The question is, what is the phase?

To answer the question we enter the experimental result onto the graph depicting the normalized volume V/V_0 versus c/a along the EBP (Fig. 1, bottom panel). From the parameters listed above we calculate $c = d_{\text{bulk}} \times 2 = 4.70 \pm 0.10 \text{ \AA}$, hence with $a = 3.1652 \text{ \AA}$ we get $c/a = 1.48 \pm 0.04$. The vol-

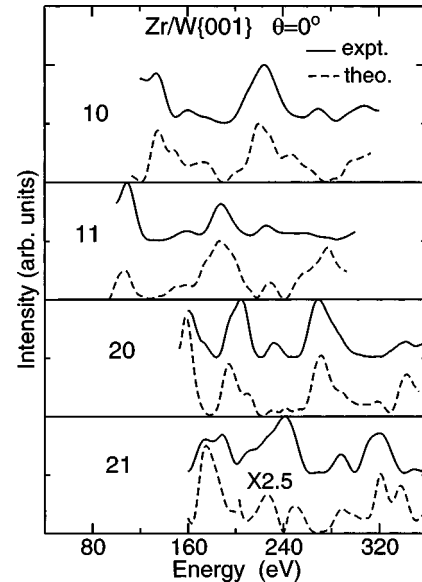


FIG. 2. Experimental (solid) and theoretical (dashed) $I(V)$ curves from a Zr film grown pseudomorphically on W{001}.

ume per atom is $V = ca^2/2 = 23.54 \pm 0.51 \text{ \AA}^3$. For the reference volume V_0 we take the experimental volume of the hcp ground state of Zr, namely, $V_0 = 23.27 \text{ \AA}^3$, whence $V/V_0 = 1.012 \pm 0.022$. We then enter the point with the c/a and V/V_0 values just found in Fig. 2, bottom (open circle). The experimental point is clearly close to the calculated fcc point on either the LDA or the GGA curve, from which we conclude that the Zr film grown or annealed at 200 $^{\circ}\text{C}$ has a structure strained (by the pseudomorphism) from the fcc phase.

This result confirms the existence of a metastable fcc phase of Zr, and is in this respect in agreement with the results of CRD (Ref. 2) and of Hill *et al.*³ But the details are discordant. CRD found that deposits on room-temperature substrates were amorphous, whereas we (and Hill *et al.*) found them to be crystalline with a 1×1 net. Moreover, it is not clear why CRD could grow very thick films of fcc Zr on substrates which apparently did not favor pseudomorphism, namely, mica (monoclinic with $a = 5.20$, $b = 9.03$, and $c = 20.11 \text{ \AA}$ and $\beta = 95.78^{\circ}$), rocksalt ($a = 5.6 \text{ \AA}$), and glass (amorphous). In all three cases the fcc phase was apparently *not* constrained, yet it grew very thick and did not collapse to hcp even at high temperatures and in relatively poor vacuum—a surprising behavior for a *metastable* phase. In our experiments the fcc phase *was* constrained and was therefore expected to stabilize at least for some thickness in a strained form. However, it is surprising that with a misfit of only 0.15%, which would give small strains, the growing Zr film had obviously many defects (shown by the high LEED background).

The comparison with the work of Hill *et al.*³ is also not wholly satisfactory. These authors used a W substrate, as we did, and observed *two* 1×1 structures with different in-plane parameters, one after thick depositions, which persisted stably even after anneals to 1300 $^{\circ}\text{C}$, and another when “islands” grew “smoothly out of the 1×1 layer,” the latter then

was identified to be fcc Zr. We also observed two 1×1 structures, but with the *same* in-plane lattice constant, one after deposition on the unheated substrate, and another after deposition on the substrate heated to 200 °C, the latter identified as strained fcc. The former converted to fcc when annealed to 200 °C.

These discrepancies remain unexplained. We can only conclude that the agreement between our findings and those of CRD and Hill *et al.* is limited to the fact that fcc Zr can be grown epitaxially in the form of thin films.

Our calculations of the EBP have also produced some surprises, namely, (i) we found an EBP with *three* energy minima, with both the LDA and GGA; (ii) we established that fcc, bcc, and bct Zr are all metastable for the LDA, but that bcc Zr is unstable for the GGA; (iii) we found that the relative magnitudes of the energy minima are different for the LDA and GGA: bct Zr has lower energy than both bcc and fcc Zr for the LDA, whereas fcc Zr has lower energy

than both (unstable) bcc and bct Zr for the GGA; (iv) since bcc Zr is observed at all pressures above 1133 K, it is plausible that bcc Zr is metastable at $p=0$ and $T=0$ K. Hence the LDA calculation, which finds bcc Zr to be stable, agrees better with experiment than the GGA, which finds bcc Zr unstable at $p=0$ and $T=0$ K. In any case, for the fcc phase this work has confirmed that the EBP is very useful both in the process of *finding* metastable phases as well as (in association with quantitative LEED) in the process of establishing whether that phase (or any other) has been grown in epitaxial experiments.

ACKNOWLEDGMENT

We gratefully acknowledge partial support of this work by the National Science Foundation with Grant No. DMR0089274.

¹A. R. Kutsar, *Fiz. Met. Metalloved.* **40**, 786 (1975); David A. Young, *Phase Diagrams of the Elements* (University of California, Berkeley, 1991); E. Yu. Tonkov, *High Pressure Phase Transformations—A Handbook* (Gordon and Breach, New York, 1992), Vol. 2.

²K. L. Chopra, M. R. Randlett, and R. H. Duff, *Philos. Mag.* **6**, 261 (1967).

³G. E. Hill, J. Marklund, J. Martinson, and B. J. Hopkins, *Surf. Sci.* **24**, 435 (1971).

⁴S. K. Kim, F. Jona, and P. M. Marcus, *J. Phys.: Condens. Matter* **8**, 25 (1996); P. M. Marcus and F. Jona, *ibid.* **9**, 6241 (1997).

⁵X. Z. Ji and F. Jona, *J. Phys.: Condens. Matter* **14**, 12 451 (2002).

⁶P. M. Marcus, F. Jona, and S. L. Qiu, *Phys. Rev. B* **66**, 064111

(2002).

⁷F. Jona and P. M. Marcus, *Phys. Rev. B* **63**, 094113 (2001); **65**, 155403 (2002); **66**, 094104 (2002).

⁸P. Blaha, K. Schwarz, and J. Luitz, Computer code WIEN97 (Vienna University of Technology, Vienna, Austria, 1997). [Improved and updated UNIX version of the original copyrighted WIEN code which was published by P. Blaha, K. Schwarz, P. Sorantin, and S. B. Trickey, in *Comput. Phys. Commun.* **59**, 399 (1990).]

⁹D. W. Jepsen, *Phys. Rev. B* **22**, 814 (1980); **22**, 5701 (1980).

¹⁰V. L. Moruzzi, J. F. Janak, and A. R. Williams, *Calculated Electronic Properties of Metals* (Pergamon, New York, 1978).

¹¹E. Zanazzi and F. Jona, *Surf. Sci.* **62**, 61 (1977).